Original Article

High Performance Polymers

High Performance Polymers
2016, Vol. 28(2) 140–146

DOI: 10.1177/0954008315572493
hip.sagepub.com

Synergistic effects of nano-silica on aluminum diethylphosphinate/ polyamide 66 system for fire retardancy

Zhaoshun Zhan[1,2], Bin Li[1,2], Miaojun Xu[1] and Zhanhu Guo[3]

Abstract

Nano-silica had been used as a synergistic agent for the preparation of aluminum diethylphosphinate (AlPi) flame retardant polyamide 66 (PA66/AlPi) and PA66/AlPi/nano-silica composites through twin-screw extrusion. The limiting oxygen index (LOI), used to characterize the minimum amount of oxygen needed to sustain a candle-like flame, revealed that the PA66/10%AlPi/1%nano-silica composites exhibited an excellent flame retardant efficiency with a high LOI value of 32.3%. The vertical flame test (UL-94) revealed that the PA66/10%AlPi/1%nano-silica composites passed the V-0 rating without drop melting. Cone calorimeter test revealed that the heat release rate and total heat rate for the PA66/10%AlPi/1%nano-silica composites were significantly decreased by 51.1 and 16.8%, respectively, compared with those of pure PA66. The thermogravimetric analysis showed that the PA66/10%AlPi/1%nano-silica composites had vast chars of 8.1% even at 800°C, indicating that nano-silica could promote the char formation of the PA66 composites. Scanning electron microscopy indicated a solid and tough residue of the burned PA66/10%AlPi/1%nano-silica composites as compared with the very loose and brickle residue of the burned pure PA66, indicating that a suitable amount of nano-silica played a synergistic effect in the flame retardancy.

Keywords

Polyamide 66, flame retardancy, aluminum diethylphosphinate, nano-silica

Introduction

Polyamide 66 (PA66) serving as a kind of engineering thermoplastic plays an important role in modern industrial fields.[1–4] PA66 is endowed with unique properties such as high tensile strength, high ductility, good chemical resistance, good abrasion, low friction coefficient, good electrical insulating, and easy processing.[5–9] However, some disadvantages of PA66 limiting its applications include poor dimensional stability, high moisture absorption, low heat-deflection temperature, and easy flammability.[10–14] Among all these disadvantages, the vital drawback of PA66 is its high flammability. Among many researched flame retardants on PA66, the halogen-containing flame retardants have been limited in the polymeric materials due to the release of corrosive and toxic products during the combustion process.[15–17]

Nowadays, advanced halogen-free flame retarded systems have attracted increasing attention in the flame retardation of materials.[18] The most promising halogen-free flame retardants are phosphorus-based organic or inorganic compounds. The developed and commercialized metal phosphinates[19,20] belong to a novel class of phosphorous flame retardants, such as aluminum diethylphosphinate (AlPi).[21,22] However, AlPi causes some processing problems and decreases the intrinsic properties of the polymers, since the required AlPi loading is usually very high (typically more than 15 wt%). For example, Braun et al.[23] have reported that AlPi (18 wt%) was incorporated into PA66 to manufacture the glass fiber-reinforced PA66 composites

[1] Heilongjiang Key Laboratory of Molecular Design and Preparation of Flame Retarded Materials, College of Science, Northeast Forestry University, Harbin, China
[2] Key Laboratory of Bio-based Material Science and Technology, Northeast Forestry University, Ministry of Education, Harbin, China
[3] Integrated Composites Laboratory (ICL), Chemical and Biomolecular Engineering Department, University of Tennesse, Knoxville, TN, USA

Corresponding author:
Bin Li, Heilongjiang Key Laboratory of Molecular Design and Preparation of Flame Retarded Materials, College of Science, Northeast Forestry University, Harbin, China.
Email: libinzh62@163.com

and the thermal stability was increased. Ramani et al.[24] have reported the excellent flame retardancy in the polyamide composites with the combination of AlPi (18 wt%) and the melamine polyphosphate. The loading of AlPi was pretty high. In order to reduce the dosage and to enhance the fire retardation of AlPi, some synergistic nanoparticles have been incorporated into polyamide together with AlPi.[25–31] However, there is no report about the AlPi with the combination of nano-silica to enhance the flame retardancy of PA66 and to reduce the loading of AlPi.

In this work, nano-silica[32–35] was used as the synergistic agent[36,37] and combined with AlPi to modify PA66. The flame retardancy of the composites was characterized by the limiting oxygen index (LOI) and vertical flammability test. The oxidative thermal degradation was studied by thermogravimetric analysis (TGA). The burning behavior was evaluated by a cone calorimeter (CONE). The evolution of surface morphologies of pure PA66 and its nanocomposites with optimal combination after CONE test were studied using a field emission scanning electron microscope (SEM).

Experimental

Materials

PA66 (101L) was supplied by DuPont Company Ltd. (Wilimington, Del., USA). AlPi was offered by Tianjin Zhenxing Chemicals Company, China, and nano-silica (200 nm) was supplied by Jinan Denuo Chemical Material Co., Ltd, China.

Preparation of PA66/AlPi/nano-silica composites

The PA66 composites with 14.0, 10.0 wt% AlPi, and 10 wt% AlPi plus 1.0, 3.0 and 5.0 wt% nano-silica were prepared by a twin-screw extruder (diameter (D): 20 mm, L/D: 32, Model: SLJ-20, Nanjing Jieya Chemical Engineering Equipment company, China). The temperatures from the hopper to the die at six different zones were 265, 270, 280, 280, 270, and 265°C to obtain different PA66/AlPi/nano-silica composites with a speed of 140 r min^{-1}. The extrudate was cut into pellets and dried in an oven at 80°C for 6 h. Injection molding (SJ-20 × 25, Harbin Special Plastic Product Company Ltd, China) at 280°C was used to make various specimens for testing and characterization. The ratios (w/w) of the flame retardants to PA66 are listed in Table 1.

Characterizations

The LOI values were measured on a JF-3 oxygen index meter (Jiangning Analysis Instrument Company, China) with sheet dimensions of 130 × 6.5 × 3 mm^3 according to American Society for Testing and Materials (ASTM) D2863-97. The vertical burning tests (UL-94) were carried out on a CZF-3 instrument (Jiangning Analysis Instrument Company) with sheet dimensions of 130 × 13 × 3 mm^3 according to ASTM D3801.

Table 1. The composition and flame retardancy data of the PA66 system.

Samples	Nano-silica (wt%)	LOI (%)	UL-94	
			Dripping	UL-94 rating
Pure PA66	0	21.5	Yes	–
PA66/14%AlPi	0	33.4	No	V-0
PA66/10%AlPi	0	30.5	Yes	–
PA66/10%AlPi	1	32.3	No	V-0
PA66/10%AlPi	3	35.1	No	V-0
PA66/10%AlPi	5	37.3	No	V-0

AlPi: aluminum diethylphosphinate; PA66: polyamide 66; LOI: limiting oxygen index.

TGA was carried out on a Perkin-Elmer Pyris 1 Thermal Analyzer (Waltham, Massachusetts, USA)under nitrogen atmosphere using a platinum pan containing samples of approximately 4 mg and a temperature range between 50°C and 800°C with a heating rate of 10°C min^{-1} and a gas flow of 60 mL min^{-1}.

The SEM images were observed by using a scanning electron microscop, which was provided by the Quanta 200 of FEI company. The morphological structures of the exterior layer of the char residues from CONE tests were obtained. The specimens were previously coated with a conductive layer of gold for better imaging.

A Fourier transform infrared spectrometer (FTIR) was provided by the Avatar360 of Nicolet company to examine the surface char residue after CONE test. The X-ray photoelectron spectroscopy (XPS) was carried out in an ultrahigh vacuum system equipped with a K_α hemispherical electron analyzer (Thermofisher Scienticfic Company, Waltham, Massachusetts, USA), using a monochromated aluminum Kα source, at a base pressure of 1.0×10^{-8} mbar. The carbon (C), phosphorus (P), oxygen (O), and silicon (Si) elements were analyzed.

Results and discussion

Flame retardancy of PA66/AlPi/nano-silica composites

Pure PA66 is easy to be ignited and has a low LOI value of 21.5% with no burning level in UL-94 test (Table 1). After incorporated with 14% AlPi, the LOI of PA66 was significantly increased to 33.4% and the burning level reached V-0 (short burning time and no dripping) in UL-94. With further reducing the amount of AlPi from 14 wt% to 10 wt%, the flame retardancy of PA66 was decreased obviously. The experimental results in Table 1 demonstrate that PA66 composites with AlPi could achieve higher flame retarding levels. The LOI of all the samples passed 30%

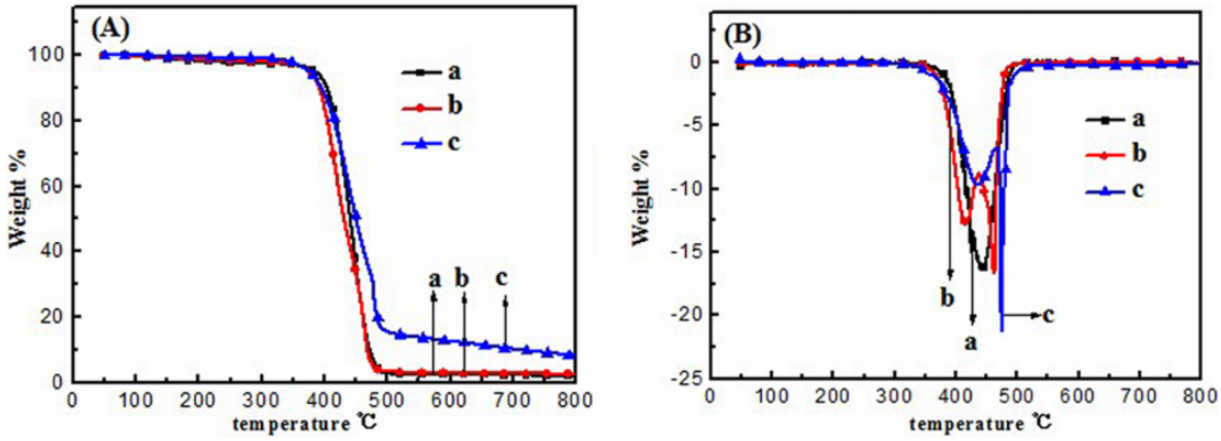

Figure 1. (a) TGA and (b) DTG curves of the PA66 system, (a′) pure PA66, (b′) PA66/14%AlPi composites, and (c′) PA66/10%AlPi/1%nano-silica composites. TGA: thermogravimetric analysis; AlPi: aluminum diethylphosphinate; PA66: polyamide 66; DTG: derivative thermogravimetry.

and the UL-94 rating achieved V-0 for pure PA66. Specially, the LOI of the PA66/10%AlPi/1%nano-silica composites reached 32.3%, indicating that AlPi could obviously increase the LOI of PA66 when it was combined with nano-silica in proper proportion (nano-silica is one percent of AlPi weight). It is observed that the LOI values were increased with increasing the loading of nano-silica at first until a maximum value of 37.3% at a loading of 5 wt% in the flame retardant. When nano-silica was used alone, the PA66 system had no UL-94 rating. After the LOI test, there was a small amount of wafery char residue of the PA66/14%AlPi composites. But combined with nano-silica, the char residue became indurative, meaning that there is a synergy between AlPi and nano-silica. Adding nano-silica as in the PA66/10%AlPi/1%nano-silica composites, the PA66 system showed the best flame retardancy and its LOI was 32.3% and its UL-94 achieved V-0 rating, meaning that AlPi has a synergy with nano-silica as well. The results show that AlPi is an excellent flame retardant for PA66 when combined with nano-silica.

TGA of the PA66/AlPi/nano-silica composites

The thermal decomposition of pure PA66 was characterized by a single decomposition step with a maximum mass loss rate at 443°C. The resulting residue was about 1.7 wt% (Figure 1, Table 2). When AlPi was added, the decomposition behavior was changed significantly. The first decomposition process was shifted to a temperature, about 28°C lower with a maximum mass loss rate at 415°C. In addition, the second part of the decomposition appeared at about 463°C. The residue at the end of the test was increased to 2.5 wt%. Similar results were described in the literature for PA66 and polyphosphate formulations in different kinds of polyamides.[23] When nano-silica and AlPi were combined in PA66, the maximal mass loss rate temperatures of the main decomposition processes of the PA66/AlPi/nano-silica composites (437 and 478°C) were higher than the ones of the PA66/AlPi composites (415 and 463°C). However, for the PA66/AlPi/nano-silica composites, no distinct separation of the decomposition processes was observed. Compared to PA66, the residue at the end of TGA experiment was clearly increased to about 8.1 wt%. The TGA results indicate a strong interaction between the additives containing phosphorus and the polymer.[38] When nano-silica and AlPi were combined, an additional preceding decomposition step was observed. The AlPi rather than nano-silica was observed to dominate the polymer decomposition. The stronger shift in the decomposition temperature typical for polyphosphate[39] did occur in the composites with combined nano-silica and AlPi.

Table 2. The TGA data of the PA66 system.

Sample	$T_{5\%}$ (°C)	T_{max1} (°C)	T_{max2} (°C)	Char yield (%)
Pure PA66	361	443	–	1.7
PA66/14%AlPi	377	415	463	2.5
PA66/%10AlPi/1%nano-silica	376	437	478	8.1

$T_{5\%}$: temperature at 5% weight loss; T_{max1}: the first maximum rate degradation temperature; T_{max2}: the second maximum rate degradation temperature; AlPi: aluminum diethylphosphinate; PA66: polyamide 66; TGA: thermogravimetric analysis.

CONE test of PA66/AlPi/nano-silica

CONE has been widely used to evaluate the flammability of materials. It can provide a wealth of information on the combustion behavior and give a measure of the size of the fire. The heat release rate (HRR) is a very important parameter and can be used to express the intensity of a fire. An effective flame retardant system normally shows a low

Table 3. The CONE data of the PA66 system.

	Pure PA66	PA66/ 14%AlPi	PA66/10%AlPi/ 1%nano-silica
IT (s)	63	49	65
Peak HRR (kW m^{-2})	1157	688	565
THR (MJ m^{-2})	113	95	94
Peak MLR (g s^{-1})	0.38	0.33	0.27
Peak SPR (m^2 s^{-1})	0.80	0.76	0.49

CONE: cone calorimeter; AlPi: aluminum diethylphosphinate; PA66: polyamide 66; HRR: heat release rate; THR: total heat rate; IT: ignition time; SPR: surface plasmon resonance; MLR: mass loss rate.

HRR value. Table 3 and Figure 2 show the data and plots of pure PA66 and its composites with and without nano-silica obtained from the CONE test at an incident heat flux of 50 kW m^{-2}. Figure 2 shows the HRR. The pure PA66 resin burns very fast after ignition and one sharp HRR peak appears with a HRR peak (peak-HRR) of 1157 kW m^{-2}. The largest amount of total heat release (THR), 113 MJ m^{-2}, was obtained (see in Figure 2). In contrast, the curves of the PA66/AlPi composites show much lower peaks and values in HRR (688 kW m^{-2}) and THR (95 MJ m^{-2}) plots; the PA66/AlPi composites with 1.0 wt% nano-silica (PA66/10%AlPi/1%nano-silica) could effectively delay the peak of HRR as the one without any nano-silica (PA66/14%AlPi). The peak-HRR (565 kW m^{-2}) was observed to appear earlier (see Figure 2). It was found that the AlPi and nano-silica obviously rendered the ignition time (IT) shortened (see Table 3), arising from the char layer formation on the surface of the PA66/AlPi composites. The char layer prevented the heat and oxygen from transferring into the matrix interior and the flammable volatiles into the flame zone. At the initial stage of heating, the surface temperature of the composite increased quickly due to the char layer formation. The increased surface temperature resulted in the fast decomposition of PA66 on the surface of the composites. Therefore, this shortened the IT. The addition of nano-silica could make this phenomenon more obvious due to the increase of the strength and stability of the char layer (shown in Figure 4). Nano-silica can also enhance the strength of char layer, prevent the char layer from cracking, enhance the

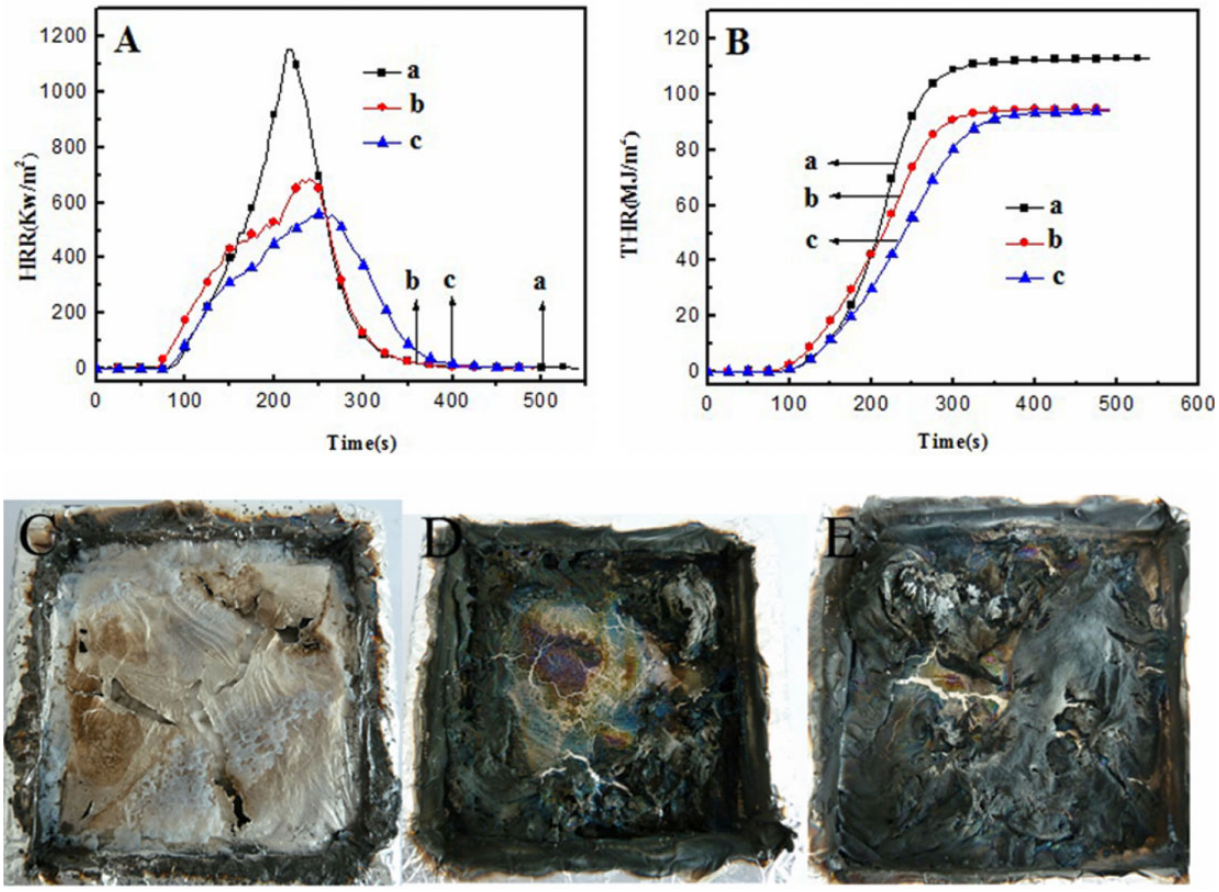

Figure 2. (a) HRR curves, (b) THR curves of (a′) pure PA66, (b′) PA66/14%AlPi composites, and (c′) PA66/10%AlPi/1%nano-silica composites, and (c), (d), and (e) digital photos of the residues after CONE test for pure PA66, PA66/14%AlPi composites and PA66/10%AlPi/1%nano-silica composites. AlPi: aluminum diethylphosphinate; PA66: polyamide 66; HRR: heat release rate; CONE: cone calorimeter; THR: total heat release.

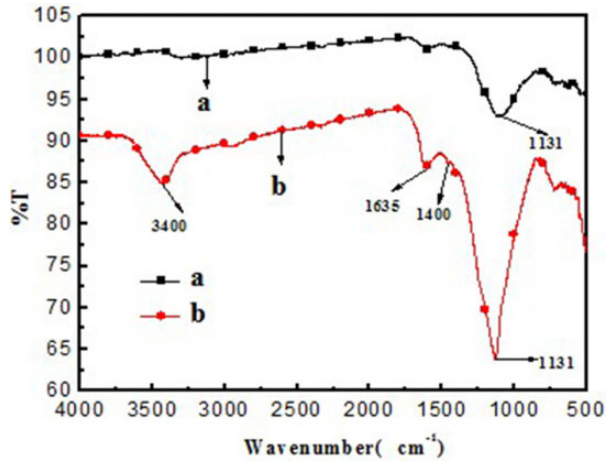

Figure 3. The FTIR spectrum of (a) the PA66/14%AlPi composites and (b) the PA66/10%AlPi/1%nano-silica composites after CONE test. AlPi: aluminum diethylphosphinate; PA66: polyamide 66; CONE: cone calorimeter; FTIR: Fourier transform infrared spectrometer.

char residue, and give a low HRR and THR. This decomposition behavior is in agreement with the TGA results as discussed above. In other words, nano-silica performed an important function as the flame retardant. This result is also attributed to the stable char layer formed.

FTIR of the PA66/AlPi/nano-silica composites char residues

In order to illustrate how the formed char affected the combustion of the PA66/AlPi/nano-silica composites, the structure of the char residues after combustion was examined by FTIR.[40] Figure 3(a) shows the FTIR spectrum of the residual for the PA66/14%AlPi composites after CONE test. The broad peaks at 3400 and 1635 cm^{-1} were attributed to the stretching of N–H groups and the peak at 1131 cm^{-1} was attributed to P=O. The broad peaks at 1400 cm^{-1} were due to the stretching of Si–-O groups. The spectrum for the PA66/10%AlPi/1%nano-silica composites given in Figure 3(b) is similar to that of the PA66/14%AlPi composites. The FTIR analysis provided positive evidence that the PA66/14%AlPi composites and the PA66/10%AlPi/1%nano-silica composites produced phosphoric and polyphosphoric acids during the thermal degradation, which served as the dehydration agents and driving force for the formation of the char layer by carbonization.

The major characteristic of a flame retardant is its ability to swell and form a strong charred layer. Figure 2 displays the digital photos of pure PA66, PA66/14%AlPi, and PA66/10%AlPi/1%nano-silica composite samples after CONE tests. The results showed that the char layer of PA66 was not formed (as shown in Figure 2(c)). But for the PA66/14%AlPi composites and the PA66/10%AlPi/1%nano-silica composite samples, a thick char layer was formed (as shown in Figure 2(d) and (e)).

SEM photographs of the PA66/AlPi/nano-silica composites char residues

Figure 4 shows the SEM micrographs of the char residue of the PA66/AlPi composites versus the loading of nano-silica. In order to elucidate the relationship between the microstructure of protective char and the flame retardancy,[41] three different kinds of char residues were collected from the CONE experiment. The char residue containing AlPi and nano-silica (Figure 4, micrographs (b) and (c)) displayed more compact structure than the one without any flame retardant (Figure 4, micrographs (a)). There were many crevasses and holes on the surface of char residue without nano-silica. Therefore, the heat and flammable volatiles could easily penetrate the char layer into the flame zone

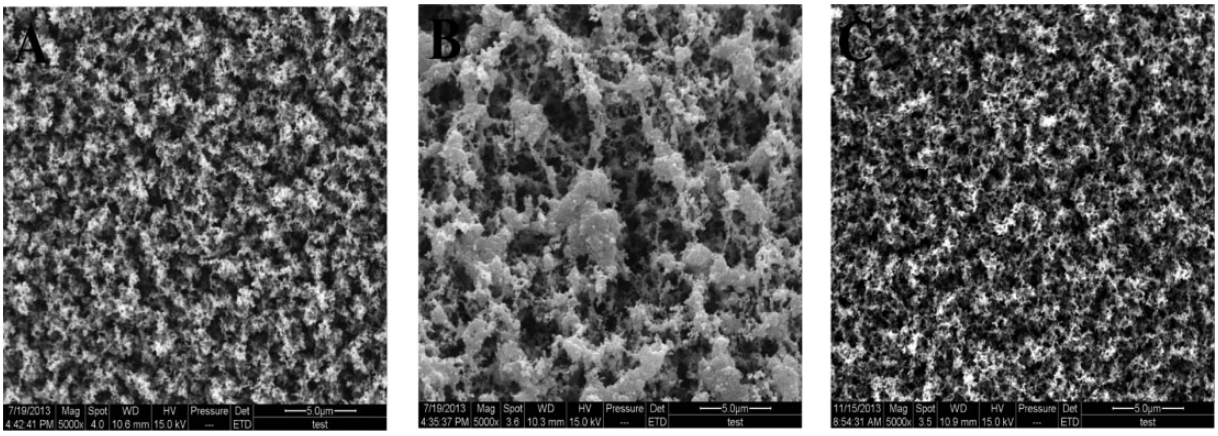

Figure 4. The SEM photographs of (a) pure PA66, (b) the PA66/14%AlPi composites, and (c) the PA66/10%AlPi/1%nano-silica composites after CONE test (5000×). AlPi: aluminum diethylphosphinate; PA66: polyamide 66; CONE: cone calorimeter; SEM: scanning electron microscopy.

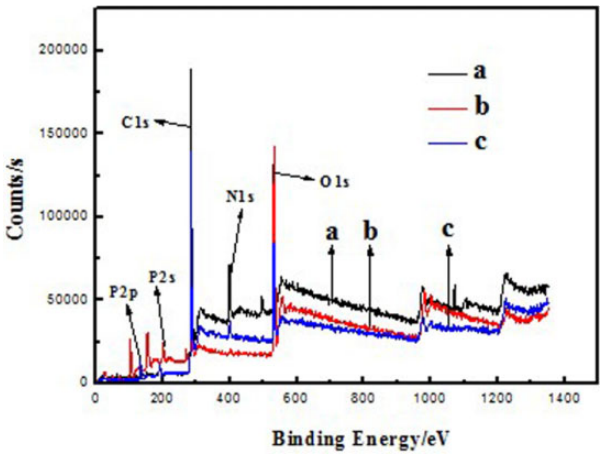

Figure 5. The XPS of (a) pure PA66, (b) the PA66/14%AlPi composites, and (c) the PA66/10%AlPi/1%nano-silica composites char residue after CONE test. AlPi: aluminum diethylphosphinate; PA66: polyamide 66; CONE: cone calorimeter; XPS: X-ray photoelectron spectroscopy.

during burning. On the contrary, the char residue surface containing nano-silica almost had no flaw, and the char layer seemed thicker and more solid than the former, which might effectively stop the transfer of the heat and flammable volatiles to give a better flame retardancy.

XPS of the PA66/AlPi/nano-silica composites char residues

XPS is an effective measurement technique to study the surface chemical structure of the samples without destruction. The chemical compositions of the outer residual char surface of pure PA66, PA66/14%AlPi, and PA66/10%AlPi/1%nano-silica composites after CONE testing were analyzed by XPS. Figure 5 shows the XPS spectra and the relative content of the outer residual char surface for pure PA66, PA66/14%AlPi, and PA66/10%AlPi/1%nano-silica composites. The peaks at 134.08, 190.90, 284.56, 400.22, and 532.71 eV can be assigned to P2p, P2s, C1s, N1s, and O1s of chars, respectively. The relative content of C, Si, and P for the outer char surface of the PA66/10%AlPi/1%nano-silica composites is much higher than those of the PA66/14%AlPi composites. The change of the above relative content is due to the presence of 1.0 wt% nano-silica, indicating that nano-silica can retain more O, N, and P in the outer and inner char surfaces to improve the strength of char.

Conclusions

The PA66/AlPi/nano-silica composites show excellent flame retardancy and anti-dripping resistance for the PA66 composites with combined AlPi and nano-silica. There is a synergistic effect between AlPi and nano-silica that gives PA66 a LOI value of 31.9% and UL-94 V-0 rating. With the optimum flame retardant formulation, PA66 has the lowest peak-HRR, THR, surface plasmon resonance values, and the most char residue in all the selected samples. Moreover, the char surface properties characterized by SEM micrograph prove that not only quantity but also quality of the char formed during the burning are crucial to the flame retardancy and anti-dripping ability of the PA66 system.

Declaration of Conflicting Interests

The author(s) declared no potential conflicts of interest with respect to the research, authorship, and/or publication of this article.

Funding

The author(s) disclosed receipt of the following financial support for the research, authorship, and/or publication of this article: The financial support of this work under the Fundamental Research Funds for the Central Universities (2572014AB19) is gratefully acknowledged.

References

1. Arif MF, Meraghni F, Chemisky Y, et al. In situ damage mechanisms investigation of PA66/GF30 composite: effect of relative humidity. *Compos Part B-Eng* 2014; **58**: 487–495.
2. Chen J, Wu W, Chen C, et al. Toughened nylon66/nylon6 ternary nanocomposites by elastomers. *J Appl Polym Sci* 2010; **115**(1): 588–598.
3. Kalkan ZS and Goettler LA. In situ polymerization of polyamide 66 nanocomposites utilizing interfacial polycondensation. II. Sodium montmorillonite nanocomposites. *Polym Eng Sci* 2009; **49**(9): 1825–1831.
4. Kalkan ZS and Goettler LA. In situ polymerization of polyamide 66 nanocomposites utilizing interfacial polycondensation. III. Co-synthesis of silica nanocomposites via sol-gel chemistry. *Polym Eng Sci* 2012; **52**(11): 2410–2416.
5. Kanno T, Yanase H, Sugata Y, et al. Flame resistant nylon-6,6 composites with improved mechanical strength by the combination of additive- and reactive-type flame retardants. *Polym J* 2007; **39**(4): 347–358.
6. Kim SR. Thermal diffusivity of in-situ exfoliated graphite intercalated compound/polyamide and graphite/polyamide composites. *Express Polym Lett* 2012; **6**(6): 476–484.
7. Li L, Li B, and Tang F. Influence of maleic anhydride-grafted EPDM and flame retardant on interfacial interaction of glass fiber reinforced PA-66. *Eur Polym J* 2007; **43**(6): 2604–2611.
8. Agrawal S, Singh KK, and Sarkar P. Impact damage on fibre-reinforced polymer matrix composite – A review. *J Compos Mater* 2013; **48**(3): 317–332.
9. Almusallam TH, Al-Salloum YA, Alsayed SH, et al. Tensile properties degradation of glass fiber-reinforced polymer bars embedded in concrete under severe laboratory and field environmental conditions. *J Compos Mater* 2013; **47**(4): 393–407.
10. Mohaddes F, Wang L, Shanks RA, et al. Elevation of charring level of polyamide-6,6 films via ionic introduction of phosphoric acid and boric acid esters. *Green Chem Lett Rev* 2014; **7**(2): 184–190.

11. Mouhmid B, Imad A, Benseddiq N, et al. A study of the mechanical behaviour of a glass fibre reinforced polyamide 6,6: experimental investigation. *Polym Test* 2006; **25**(4): 544–552.
12. Qin H, Su Q, Zhang S, et al. Thermal stability and flammability of polyamide 66/montmorillonite nanocomposites. *Polymer* 2003; **44**(24): 7533–7538.
13. Seefeldt H, Duemichen E, and Braun U. Flame retardancy of glass fiber reinforced high temperature polyamide by use of aluminum diethylphosphinate: thermal and thermo-oxidative effects. *Polym Int* 2013; **62**(11): 1608–1616.
14. Wang H, Wang L, Wang R, et al. Design and synthesis of the polyaniline interface for polyamide 66/multi-walled carbon nanotube electrically conductive composites. *Colloid Polym Sci* 2012; **291**(4): 1001–1007.
15. Li B, Zhan Z, Zhang H, et al. Flame retardancy and thermal performance of polypropylene treated with the intumescent flame retardant, piperazine spirocyclic phosphoramidate. *J Vinyl Addit Technol* 2014; **20**(1): 10–15.
16. Bourbigot S, Cerin O, Duquesne S, et al. Flame retardancy of bitumen: a calorimetry study. *J Fire Sci* 2013; **31**(2): 112–130.
17. Farsadi M, Öchsner A and Rahmandoust M. Numerical investigation of composite materials reinforced with waved carbon nanotubes. *J Compos Mater* 2013; **47**(11): 1425–1434.
18. Weil ED and Patel NG. Iron compounds in non-halogen flame-retardant polyamide systems. *Polym Degrad Stab* 2003; **82**(2): 291–296.
19. Li H, Ning N, Zhang L, et al. Different flame retardancy effects and mechanisms of aluminium phosphinate in PPO, TPU and PP. *Polym Degrad Stab* 2014; **105**(3): 86–95.
20. Doğan M and Bayramlı E. The flame retardant effect of aluminum phosphinate in combination with zinc borate, borophosphate, and nanoclay in polyamide-6. *Fire Mater* 2014; **38**(1): 92–99.
21. Horrocks AR, Smart G, Hörold S, et al. The combined effects of zinc stannate and aluminium diethyl phosphinate on the burning behaviour of glass fibre-reinforced, high temperature polyamide (HTPA). *Polym Degrad Stab* 2014; **104**(3): 95–103.
22. Yan Y, Huang J, Guan Y, et al. Flame retardance and thermal degradation mechanism of polystyrene modified with aluminum hypophosphite. *Polym Degrad Stab* 2013; **99**(12): 35–42.
23. Braun U, Schartel B, Fichera MA, et al. Flame retardancy mechanisms of aluminium phosphinate in combination with melamine polyphosphate and zinc borate in glass-fibre reinforced polyamide 6,6. *Polym Degrad Stab* 2007; **92**(8): 1528–1545.
24. Ramani A and Dahoe AE. On flame retardancy in polycaprolactam composites by aluminium diethylphosphinate and melamine polyphosphate in conjunction with organically modified montmorillonite nanoclay. *Polym Degrad Stab* 2014; **105**(3): 1–11.
25. Mistretta MC, Morreale M, and La Mantia FP. Thermomechanical degradation of polyethylene/polyamide 6 blend-clay nanocomposites. *Polym Degrad Stab* 2013; **99**(12): 61–67.
26. Bellucci F, Camino G, Frache A, et al. Catalytic charring–volatilization competition in organoclay nanocomposites. *Polym Degrad Stab* 2007; **92**(3): 425–436.
27. Jang BN, Costache M, and Wilkie CA. The relationship between thermal degradation behavior of polymer and the fire retardancy of polymer/clay nanocomposites. *Polymer* 2005; **46**(24): 10678–10687.
28. Jang BN and Wilkie CA. The effect of clay on the thermal degradation of polyamide 6 in polyamide 6/clay nanocomposites. *Polymer* 2005; **46**(10): 3264–3274.
29. Karamipour SH, Ebadi-Dehaghani H, Hajari M, et al. Comparing the effect of micro- and nano-scale silica on the rheological, dynamic mechanical properties and flame resistance of nylon 6,6. *J Macromol Sci B* 2014; **53**(9): 1574–1590.
30. Kashiwagi T, Harris RH, Zhang X, et al. Flame retardant mechanism of polyamide 6–clay nanocomposites. *Polymer* 2004; **45**(3): 881–891.
31. Kaynak C and Ibibikcan E. Contribution of nanoclays to the flame retardancy of polyethylene-based cable insulation materials with aluminum hydroxide and zinc borate. *J Fire Sci* 2013; **32**(2): 121–144.
32. Pan M, Mei C, Du J, et al. Synergistic effect of nano silicon dioxide and ammonium polyphosphate on flame retardancy of wood fiber–polyethylene composites. *Compos A-Appl S* 2014; **66**(7): 128–134.
33. Kiliaris P and Papaspyrides CD. Polymer/layered silicate (clay) nanocomposites: an overview of flame retardancy. *Prog Polym Sci* 2010; **35**(7): 902–958.
34. Yagnamurthy S, Chen Q, Chen C, et al. Erosion yield of epoxy–silica nanocomposites at the lower earth orbit environment of the International Space Station. *J Compos Mater* 2013; **47**(1): 107–117.
35. Florea NM, Lungu A, Vasile E, et al. The influence of nanosilica functionalization on the properties of hybrid nanocomposites. *High Perform Polym* 2012; **25**(1): 61–69.
36. Su X, Yi Y, Tao J, et al. Synergistic effect between a novel triazine charring agent and ammonium polyphosphate on flame retardancy and thermal behavior of polypropylene. *Polym Degrad Stab* 2014; **105**(7): 12–20.
37. Guo Z, Li H, Liu Z, et al. Preparation, characterization and thermal properties of titanium- and silicon-modified novolac resins. *High Perform Polym* 2012; **25**(1): 42–50.
38. Samyn F and Bourbigot S. Thermal decomposition of flame retarded formulations PA6/aluminum phosphinate/melamine polyphosphate/organomodified clay: Interactions between the constituents? *Polym Degrad Stab* 2012; **97**(11): 2217–2230.
39. Jimenez M, Duquesne S, and Bourbigot S. Enhanced fire retardant properties of glass-fiber reinforced Polyamide 6,6 by combining bulk and surface treatments: toward a better understanding of the fire-retardant mechanism. *Polym Degrad Stab* 2013; **98**(7): 1378–1388.
40. Ramani A, Hagen M, Hereid J, et al. Interaction of a phosphorus-based FR, a nanoclay and PA6-Part 1: interaction of FR and nanoclay. *Fire Mater* 2009; **33**(6): 273–285.
41. Schartel B, Bartholmai M, and Knoll U. Some comments on the main fire retardancy mechanisms in polymer nanocomposites. *Polym Advan Technol* 2006; **17**(9): 772–777.